Synchronised WindScanner Field Measurements of the Induction Zone Between Two Closely Spaced Wind Turbines

Anantha Padmanabhan Kidambi Sekar, Paul Hulsman, Marijn Floris van Dooren and Martin Kühn

December 18, 2023

Reviewer 2

This paper presents some unique results of dual-Doppler retrieval of wind field in the induction zone of a turbine subject to different wake conditions. This work is novel and quite relevant, but some important changes, especially to the physical explanations provided to the observed phenomena, are necessary.

We thank the reviewer for their critical assessment of our work. In the following, we address the concerns point by point. We hope these changes will positively benefit the manuscript. Comments to the reviewer points are made in blue while modifications to the manuscript are made in red.

Based on the comments of Reviewers 1, 2 we have summarised the major changes in the revised manuscript below:

- Expanded the site characterisation section with the topography and the presence of flow blockage (treeline) in between the two turbines and the discussion section to include the effects of the topography and treeline as a possible explanation for our measured flow features and a discussion on how to decouple the terrain effects from the rotor aerodynamic effects.
- Updated the LES results section with an analysis of the statistical uncertainty of the measurements.
- Expanded the LES Results section to include the rationale behind our assumption of the vertical velocity on the Standard Uncertainty Propagation (SUP) and its impact on the width of error bars. The discussion section has been updated to include the significance of our results based on the SUP assumptions and suggestions for future measurements with a third synchronised lidar.
- The conclusion section has been reworked substantially to include a description of our measurements, measured flow features, a summary of the uncertainty analysis and summary of challenges in conducting field measurements for obtaining validation data for numerical models.

General Comments

Comment 1: The error analysis is very accurate but some results of it may be misrepresented. SUP and LES do not include all the sources of error, as correctly indicated in Table 2. This should

be reiterated when commenting, for instance, Fig. 9 to make sure the reader does not interpret the error bands based on SUP as an estimate for the limits of the difference of the LES validation. For instance, the error band around v is significantly larger than the difference shown by LES but simply due to the lack of pointing accuracy in LES.

Reply: Indeed, SUP and LES does not contain all sources of errors, which is why we had used both methods for our analysis. In the revised manuscript, we have clearly specified the method through with the error bars were obtained and expanded the discussion accordingly.

We have added the similar text to the revised manuscript in Section 3.1.2 to the measurement cases. The error bars around the v component profiles are larger than the differences in the LES and WindScanner resolved profiles due to the inclusion of multiple error terms in the SUP.

Comment 2: Also, not including statistical uncertainty in the following plot may be misleading as this last contribution can easily dominate the overall uncertainty in real experimental campaigns. Statistical uncertainty and convergence are discussed in Section 2.3.2 but the simple comparison with the work of Simley et el. 2016 is not sufficient to justify the current results. The statistical uncertainty is a function of the specific flow conditions (mostly turbulence intensity and integral timescale) as well as number of samples. Please add at least an estimate of the error on the mean to make sure it is ok to neglect it compared to the other uncertainties.

Reply: We agree with the reviewer that the statistical uncertainty needs to be presented. While the total propagated uncertainty regards the accuracy of single input variables, the statistical uncertainty quantifies the precision of the results from different scans. A higher number of scans typically reduces measurement noise from the statistical error. To quantify the statistical uncertainty, we use the margin of error estimated in the scanning area, for the LES case with two aligned and operational turbines. The margin of error was calculated as $e_{\mathrm{u,stat}} = \frac{z_\gamma \sigma_\mathrm{u}}{\sqrt{N_\mathrm{s}}}$ and $e_{\mathrm{v,stat}} = \frac{z_\gamma \sigma_\mathrm{v}}{\sqrt{N_\mathrm{s}}}$. Here z_γ, the confidence level, is set to 1.96, denoting the 95 % confidence interval, $\sigma_\mathrm{u}, \sigma_\mathrm{v}$ are the standard deviations of the longitudinal and lateral velocity components in the scan plane obtained from the WindScanner simulations and N is the number of samples.

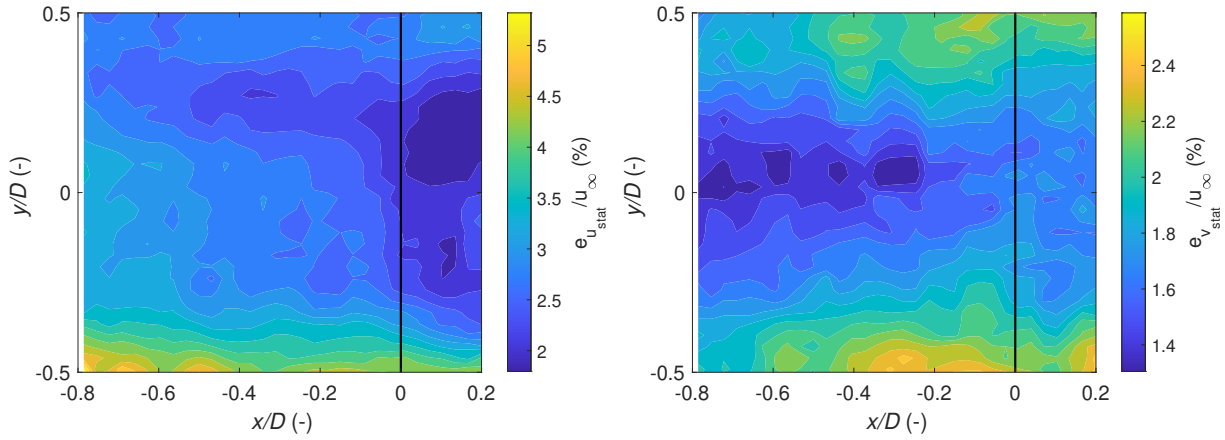

Figure 1: Statistical Uncertainty estimated for the u, v components.

Figure 1 shows the variation of the margin of error in the scanning area for the two reconstructed components normalised with the mean longitudinal wind speed. The margin of error for the longitudinal component varies in the scan area between 2 % to 5 % depending on the turbulence intensity in the wake. Similarly, for the v- component, the margin of error varies between 1.3 % and 2.5 %. The higher errors at scan edges could be attributed to the low amount of data points in these locations as a consequence of the scanning patterns. This indicates that our set-up can capture the averaged velocities in the scan plane with a statistical uncertainty that is lower than the dual-Doppler propagated uncertainties. In the field data, we can expect that the margin of error would be slightly higher than in the idealised LES due to the filtering procedure reducing data availability in each scan.
We have added the presented analysis of the statistical uncertainty in Section 3.1 of the revised manuscript.

Comment 3: A major drawback is also discussing differences in the measurements that are much smaller than the associated uncertainty (e.g. Fig. 16 and 17). The claimed "asymmetries" in the yaw steering cases are not significant enough to be considered a physical feature. The uncertainty quantification must indeed be used to flag significance of the results, otherwise it becomes just a theoretical exercise. Please either mention that the observed small differences between cases 3 and 4 are not relevant (so everything is really speculative) or remove at all Fig. 16 and 17 and the associated discussion.

Reply: We acknowledge that we have not discussed the significance of the results in detail. We first discuss the methodology by which the error bars were drawn in Fig 16, and 17 before suggesting a way linking the uncertainty quantification exercise and the measurements.
The error bars in Figs. 14, 16, and 17 were estimated using a w component value of 1 m/s. We acknowledge that the reasoning behind the choice of w velocities for the SUP method was not detailed in the paper. In the LES analysis, the reference wind fields provided an accurate value of the local w component variation inside the scanning area. This local w velocity was subsequently used to calculate the propagated uncertainties providing a methodology to investigate the lidar error inside the LES. However, in the free field, we did not have any measurements of the local w component. Therefore, an assumption of a constant w was required for the Standard Uncertainty Propagation (SUP) methodology. For the full wake and partial wake cases, a value of $w = 1$ m/s was assumed, similar to the wind tunnel experiments of van Dooren et al [15]. For the undisturbed inflow case, the vertical velocity would be only dominated by the temperature flux between the ground and the air, and therefore a conservative value of $w = 0.2$ m/s was chosen based on the weakly stable conditions during the measurements.
The assumption of constant w velocities in the measurement plane for SUP calculations will have a significant impact on our results. Therefore, the errors would be overestimated at locations where the local w component would be low, for instance, the most upstream part of the scan where the aerodynamic influence of the rotor on the flow would not be felt by the wind field. To illustrate this we plot the variation of e_u and e_v in the scanning area for the LES case with an assumption of $w = 1$ m/s in Figure 2.
The comparison of e_u and e_v for the two methods indicates two things. Firstly, assuming constant w on the scanning area masks the velocity reconstruction error that is dependent on the flow dynamics, especially close to the rotor. Secondly, the magnitude of e_u and e_v for the constant w velocity case is substantially larger than the errors estimated using the local w velocities. The consequence of this is that the presented error bars in Figures 11, 14, 16 and 17 of the original manuscript are conservative, leading to difficulties in the interpretation and significance of the results. Had the w component been low, the

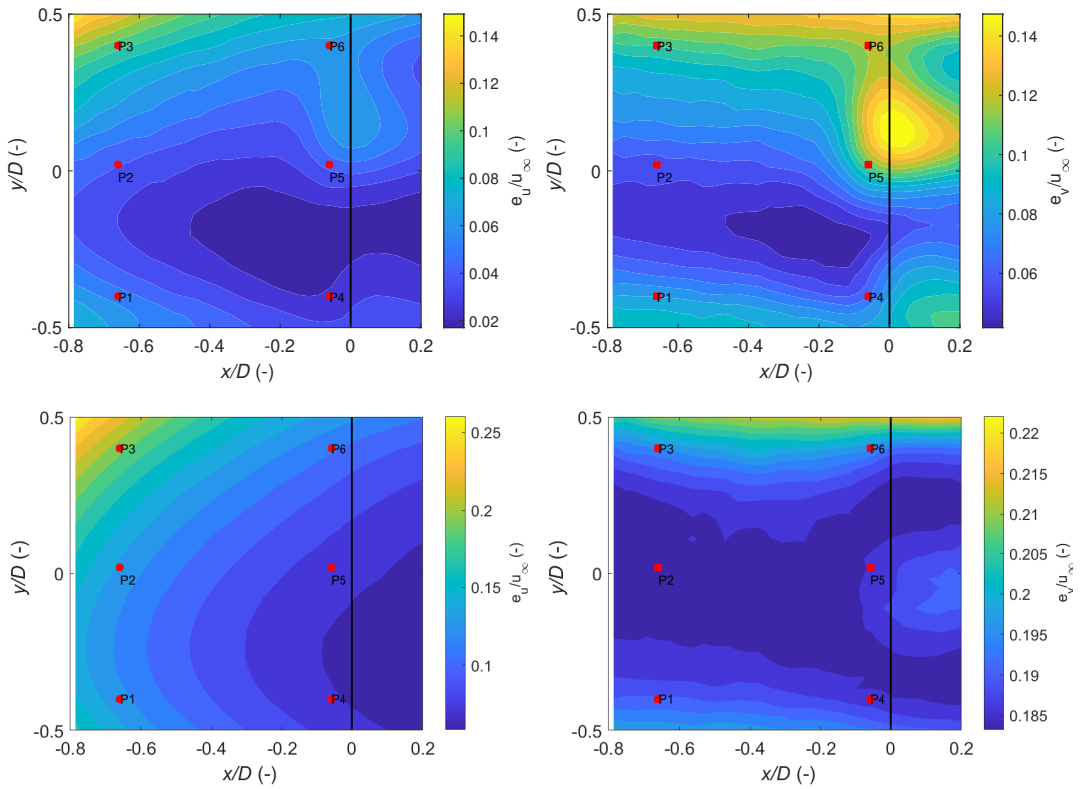

Figure 2: Variation of e_u and e_v in the scanning area using the assumption of $w = 1$ m/s (bottom row) and the local w component from the LES (top row).

error bars could have been smaller and we could have made definitive statements on the significance of the results. In the revised version of the paper, we have shown and discussed the spatial variation of the propagated error using the actual and assumed vertical velocities to bridge the LES and the field measurements. We have extended the discussion section, highlighting the assumption and its impact on the significance and interpretation of the measurements. A possible workaround would have been to use a third synchronised lidar that would eliminate the assumption of vanishing vertical velocity, however, a third system was not available for measurements. We acknowledge this unavoidable limitation of our measurement setup and have made the following changes in the manuscript.

We have made the following changes in the revised manuscript.

- Expanded the LES Section 3.1 with the SUP analysis based on the assumptions of w velocity instead of the true LES velocities to link the simulations and experiments.
- Extended the discussion section, highlighting the assumption and its impact on the significance and interpretation of the measurements.

Comment 4: A major issue with the interpretation of the results concerns the observer asymmetry of the induction zone. First, a mild asymmetry seems to show in the LES results, but on the other side of the rotor (Fig 6) compared to the lidar observation. Please explain why this is

the case. Second and foremost, the physical explanation provided for this asymmetry, namely the "different angles of attacks" between the left and right side of the rotor induced by "wind shear" is not clear. If we consider the same height AGL, then the incoming wind speed is the same on both sides of the rotor. Being the rotational speed the same, this results in identical local inflow, relative speed and angle of attack. Furthermore, it was not found any evidence in the cited references supposedly reporting such effect. The cited papers do indeed show symmetrical induction zones even with shear, as it should be. If there's a fundamental mechanism creating this asymmetry, please provide a schematic with the angles of attacks as a function of the blade position.

Reply:

In our attempt to explain the measurements, we first will discuss the quality of the collected data and then proceed with an explanation for the measurement results. We are confident in the ability to achieve the scanning trajectories with high accuracy through extensive wind tunnel and field testing. Therefore, we could eliminate any mechanical/optical issues with the lidars that would contaminate measurements.

We referred to the work of Bastankah et al [2] who conducted wind tunnel measurements of a model wind turbine under sheared conditions ($\alpha = 0.17$). They noted "a slight lateral asymmetry with respect to the rotor axis" visualised through iso-velocity contours at far upstream positions. Similar to our measurements, the asymmetry also disappears closer to the rotor plane. Bastankah et al provided a possible explanation of the slight asymmetry due to rotor blades experiencing different angles of attack as they move through the sheared flow. However, as pointed out, indeed the induced velocities for a rotor with a constant rpm will be the same on either side of the rotor and will only change the induction in the vertical direction. This is the effect that we wanted to describe with the work of Frosting et al [9] who show the variation of induction in the rotor plane for strongly sheared flow. We also described the mechanism of momentum transfer between the lower and upper parts of the rotor as an additional explanation for the asymmetry. The authors thank the reviewer for pointing us towards the work of Madsen et al [8] who provided similar reasoning of the wake rotation and its impact on the induced velocities at the rotor plane.

However, as noted by Reviewer 1, we had not fully characterised the test site in terms of terrain which could provide additional explanation for the measured asymmetry. The induction zone behaviour can be mischaracterised with observations if the effects of nonuniform terrain on the flow are not carefully considered. This non-uniformity could be a result of the changing terrain upstream of the turbine or the presence of a forest or a tree line. For instance, Mikkelsen et al., [10] in their dual-WindScanner lidar measurements at the DTU Riso site measured a vertical velocity of 1 m/s in the induction zone which was attributed to the upward sloping terrain upstream of the turbine.

We first discuss the layout of the site more in detail, as illustrated in Fig. 3, with a spatial resolution of 200 m obtained from [3]. While the elevations at WT1 and WT2 are similar, abrupt changes in elevation are seen upstream notably the presence of a small hill with an elevation of 105 m 22 D upstream of WT1 along the predominant wind direction, creating a slope of 1.09° towards the two turbines. We also note the presence of a village, tree lines and small clumps of forested terrain along the predominant wind direction. Furthermore, a treeline exists between WT1 and WT2 and therefore in the induction region of WT2. The treeline extended towards the met mast with a height of approximately 15 m-20 m estimated from pictures taken during the installation campaign. Further analysis of the measurements from the same site was done by Hulsman et al. [7] who showed a clear effect of the same tree line by comparing the met mast and the VAD lidar data at 100 m AGL. However, the comparison is not directly transferable in our sector of interest due to the orientation of the VAD lidar and the met mast

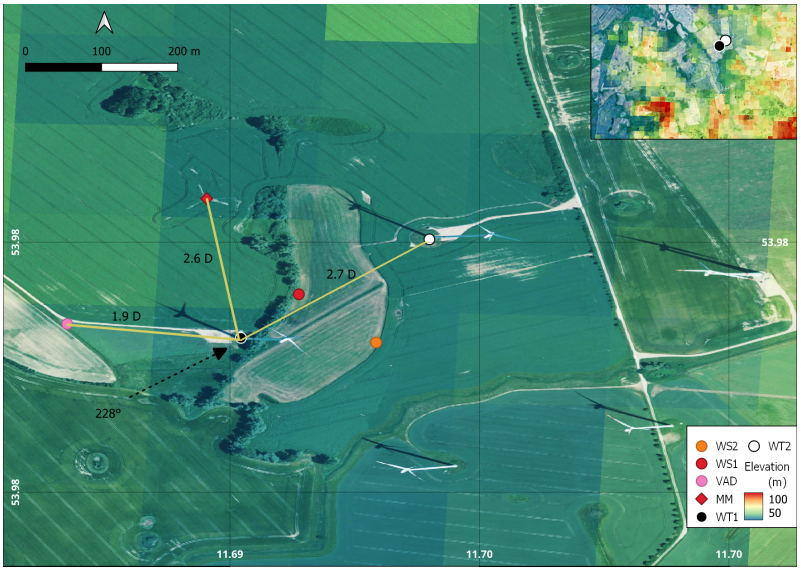

Figure 3: The wind park and measurement layout at Kirch Mulsow overlayed with elevation contours. A zoomed-out image of the site is shown in the top right corner illustrating the hills present upstream of the wind park. Here WT1, and WT2 refer to the upstream and downstream turbines, MM and VAD refer to the met mast and the inflow lidar while WS1 and WS2 refer to the two WindScanners.

but provides enough evidence of the perturbation of the flow by the treeline. This is consistent with literature where trees acting as windbreaks have been shown to perturb the vertical flow profile high above the treeline [6, 14].
We believe that the effect of terrain and in particular treeline could have influenced the flow behaviour in the induction zone, which we did not address previously. Furthermore, these effects could have also impacted the WindScanner measurements, in particular, the assumption of vanishing vertical wind speed for the dual-Doppler reconstruction which could have influenced the measurement results.
In our present setup, we could not quantify the magnitude of these terrain effects on the flow and the lidar measurements. We could not acquire measurements when both the turbines were non-operational, which would have provided insights into the flow behaviour due to terrain and the tree line. Using a high-resolution LES with a terrain map could have been used to isolate the terrain influences. However, the LES runs in our study were intended to study the lidar measurement accuracy and therefore were initialised with a roughness length as a proxy for the terrain complexity and hence not fully representative of the site. This could could explain why the asymmetry exists on the other side of the rotor compared to field measurements.
We hope that these changes to the manuscript will provide a suitable explanation for the measurements.

We have updated the test site description with the terrain map and described the treeline in between WT1 and WT2 and added the terrain and treeline effects as a possible additional effect for the flow perturbation in all the sections. We have further updated the discussion section with the effect of the terrain on the flow and the dual-Doppler reconstruction and discussed the limitation of our simulation set-up where the terrain and hence the lidar error due to terrain could not be modelled.

Specific Comments

Comment 1 — L 18, "...due to the extraction of kinetic energy by the rotor": this may be a subtlety but technically induction zones are present also around bodies that do not necessarily extract significant kinetic energy from the flow (e.g. in front of an airfoil). It is suggested rephrasing as "...due to the rotor thrust".

Reply: The sentence has been rephrased as suggested.

Comment 2 — L 57: please clarify what "assumptions of the global flow field" refers to.

Reply: The assumption of global flow field refers to the assumption of a constant vertical wind component required to perform the dual-Doppler reconstruction. We have replaced the phrasing in the paper. However, owing to the lidar measurement principle and scanning limitations, such as the volume averaging effect, assumptions of vertical velocity for dual-Doppler reconstruction, scanning speeds, beam pointing, and intersection accuracies, a thorough error and uncertainty assessment is required before interpreting the measurements

Comment 3 — Table 2: A few improvements are suggested:

- The source of the dual-Doppler error is not necessarily "Non-ideal lidar placement impacts the beam-intersection angles" as an ideal placement leading to 0 error does not exists. It is indeed an "Amplification of single-Doppler uncertainty due to dual-Doppler reconstruction".
  We have changed the text in the revised manuscript.
- The "averaging period error" could be renamed "statistical uncertainty".
  We have changed the text in the revised manuscript.
- It would be better to remove the "unavoidable" word in the description of the error due to neglecting w. In fact, one could use for instance continuity or other techniques to estimate w. Also, please explain SUP in the caption.
  We have changed the text in the revised manuscript.

Reply: We have changed the descriptions of the errors to reflect the reviewer comments and defined the abbreviations of LES and SUP on the caption.

Comment 4 — L 213: Please add reference for the dual-Doppler error (e.g. Stawiarski 2013). Also, the $\Delta\chi$ which indicates the angle between the intersecting beams which is the driving factor for the error is not the difference of the azimuth angles $\chi_1 - \chi_2$. Please clarify this point and possibly use a symbol other that $\Delta\chi$ to describe the intersection angle as χ was already used for azimuth.

Reply: We have added references to Stawiarski et al[13], van Dooren et al [16] and Pena and Mann [12] as appropriate references here. Indeed, we refer here to the intersection angle of the beams which is scales the dual-Doppler reconstruction error as described in Stawiarski et al [13]. We have represented the term as R_{int} in the revised manuscript.

Comment 5 — Table 3: A few improvements are suggested:

- Please explain all symbols in the caption.
- The stability classes indicated here do not match the three given later (stable, neutral, unstable)
- Add z/L in a new column

Reply:

- We have expanded the caption to the following:
  Summary of the measurement cases. Each case is characterised by its freestream wind speed u_∞, turbulence intensity (TI), mean wind direction (θ_{wdir}), stability parameter (z/L), stability, wind veer (γ), vertical wind shear (α_{shear}) and the yaw offset of the turbines (γ_{WT}).
- The table has been expanded to contain z/L values and the stability classes has been checked and made consistent with the results section.

Comment 6 — L 254-259: Please add justification or reference for the choice the stability classes based on L.

Reply: For justification of the choice of L for stability classification, we have added the following references to the text: .
The atmospheric stability of the boundary layer can be characterised by the Monin-Obhukov similarity theory [11, 1]. The stability parameter z/L was measured by the eddy covariance station at a height of 6 m above the ground following Bromm et al,[5].

Comment 7 — L 325-327: The details of the SUP calculation should be moved at L 314 when first introducing the figures.

Reply: We have moved the details of the SUP calculation before the figures are introduced.

Comment 8 — L 331-332: Please expand further why a high elevation leads to a high uncertainty associated with elevation. Is this just due to the structure of $\frac{\partial u}{\partial \delta}$ being proportional to δ?

Reply: The general form of the uncertainty propagation involves the product of the partial derivative and the uncertainty of the input variable, in this case, line-of-sights, beam pointing angles and vertical wind component. For the case of the elevation angle, the partial derivative $\frac{\partial u}{\partial \delta}$ was positively correlated to the elevation angle δ. Therefore, an increase in δ would result in a more substantial impact on the overall uncertainty in the wind component e_{u}. We have modified the text to the following:

At P1, P2 and P3, $e_{\delta_{\mathrm{i}}}$ is the largest contributor due to the severe elevation angles required to scan at these points and the positive correlation between $\frac{\partial u}{\partial \delta}$ and δ.

Comment 9 — L 332-333: It is also not immediately clear why the error due to neglecting w is larger for the lidar more aligned with the wind. Please clarify.

Reply: We can explain this from the contribution of the vertical velocity to the individual line-of-sight of the two lidars. For the un-aligned lidar, the lidar measures with an angle to the measurement point

and therefore the line-of-sight component will contain contributions from both the lateral and vertical velocity components. Neglecting the vertical velocity might have a smaller impact on this lidar since it already incorporates both components in its measurements. For the aligned lidar, the measurements are more sensitive to the changes in the w component. For a non-zero w component, the aligned lidar will contain a larger contribution of the w component projected onto its line-of-sight compared to the un-aligned case. We have modified the text to the following:

The varying contributions of $e_{\mathrm{w,i}}$ at the points of interest can be explained by the relative alignment of the lidar with the wind direction. For a non-zero w component, an aligned lidar will contain a larger contribution of the w component projected onto its line-of-sight compared to the un-aligned case.

Comment 10 — L 333-334: Not only P3 and P6, but also P5 has a preponderant error $e_{\mathrm{w,1}}$ which should be explained.

Reply: The error at P5 follows the same argumentation as Comment 9 and is dominated by the term $e_{\mathrm{w,i}}$. The value of $e_{\mathrm{w,1}}$ is larger than P3 and P6 due to the large local w velocity close to the rotor obtained from the LES (Fig. 6 (top right)). We have modified the text to the following:

Similarly, at P3, P5 and P6, WS1 is approximately aligned with the longitudinal wind speed component. So the errors at these points are dominated by the $e_{\mathrm{w,1}}$, which is highest at P5 due to the large local w velocity in the LES field (Fig. 06 (top right)).

Comment 11 — L 341: The location $x/D = 0.16$ is not shown in Fig 9.

Reply: Thank you for pointing this out. We have corrected the location in the text to $x/D = -0.08$ as depicted in Fig. 9.

Comment 12 — L360-361: There are several ways stable stratification could impact the induction strength, please explain why it is enhancing the velocity decrease in this case.

Reply: Stable stratification inhibits wind vertical turbulent mixing. In the induction zone, where the rotor blades are influencing the flow, stable stratification can limit the upward transport of momentum. This reduced mixing can lead to an enhancement of the induction zone and the velocity decrease. We have modified the text to the following:

This strong velocity deficit can be attributed to high axial induction and weakly stable stratification during the measurement period inhibiting vertical turbulent mixing.

Comment 13 — L367-368: It is not clear why the blades would experience different relative inflow on the left and right side of the rotor. Considering hub-height for simplicity, the inflow velocity u_{hub} is the same on both sides of the rotor if vertical shear only is present. Being the rotational component ωR necessarily the same, the velocity experienced by the blades is identical. Also, the cited reference by Meyer-Forsting shows a symmetrical behavior of the induction in their LES results (below) and is therefore inadequate. The explanation based on the interaction of wake rotation and shear is sounder [Madsen et al., 2014] at least in the near wake. Please clarify this point.

Reply: We have addressed this point in General Comment 4. Indeed the induced velocities for a rotor with a constant rpm will be the same on either side of the rotor and will only change the induction in the vertical direction. This is the effect that we wanted to describe with the work of Frosting et al [9] who show the variation of induction in the rotor plane for strongly sheared flow. We have added a further explanation of the asymmetry due to terrain effects and the presence and influence of a treeline in between WT1 and WT2.
Looking downwind, this slight asymmetry could be attributed to the presence of a tall treeline in-between WT1 and WT2 perturbing the flow and the strong vertical shear $\alpha_{\text{shear}} = 0.21$ that causes a vertical wind speed gradient varying the relative wind speed and the angle of attack of the blades during a rotation. Additionally, the induced velocities at the rotor plane are influenced by the counter-rotating wake creating a momentum transfer between the lower and upper rotor regions leading to a difference in flow magnitude between $y/D > 0$ and $y/D < 0$ [8]. Hence, the blade sections would experience varying blade forces that vary the local thrust coefficient, and hence, the induction factor and corresponding deceleration.

Comment 14 — L 380: Is the vertical velocity used only to compute uncertainty or also for the dual-Doppler reconstruction? Please explain.

Reply: The vertical velocity assumption of 0.2 m/s was chosen only for computing the uncertainty while the dual-Doppler reconstruction was done by assuming $w = 0$ m/s. Similarly, for the uncertainty assessment for the partial and full wake cases, a constant vertical velocity of 1 m/s was assumed following the work of van Dooren et al [15]. The implications of this assumption on the propagated uncertainty has been discussed in Major Comment 3. We have modified the text to the following:

For calculating the propagated uncertainties, a constant vertical component $w = 0.2$ m/s is assumed, as no wakes propagating from the non-operational upstream turbine and no direct measurements of the w component were available in the scanned area.

Comment 15 — L 388: Please clarify what the 1-96σ bounds mean. Is this the uncertainty from SUP? Why is the error bar not centered on the data?

Reply: We clarify that the error bars presented represent the propagated uncertainties from SUP and not the statistical uncertainty. The revised version of the manuscript has been updated with a plot with centred error bars on the WindScanner data.

Comment 16 — Figure 12: A deeper analysis on why FLORIS is underpredicting so drastically the induction is needed. The fact that even at the rotor plane the estimated induction is 1/3 that of other models sounds concerning. Please also provide the Ct for this case to allow other researchers to replicate the results.

Reply: We acknowledge that the systematic underprediction of the velocity deceleration's from the FLORIS model is a cause of concern and hence was not used for estimating the velocity decelerations in the partial and full wake cases. We had used the FLORIS+Induction coupling described in Branlard et al [4] that downloaded from the Github repository. We also contacted the authors of the paper [4] to describe and find a solution to the problem. The most likely reason for the discrepancy is a bug in the coupling between the induction zone models and the wake models in FLORIS. This reasoning is

supported by the good agreement between the standalone induction zone models that are used in the coupling and the field measurements.
Due to an NDA with the turbine operator, we cannot disclose the turbine Ct curve for confidentiality.

Comment 17 — L 431: Same as comment on L 380.

Reply: Please refer to Comment 14 for our answer.

Comment 18 — L 440: It is unclear what "profiles at $y/D\pm0.5$" means as those specific spanwise locations correspond to a point value in the velocity deficit, not "profiles".

Reply: We apologise for the ambiguity. We have rephrased the sentence to:
Interestingly, the spanwise velocity profiles at various upstream positions exhibits a slight asymmetry.

Comment 19 — L 442: The concept of "asymmetric induction" here is repeated and not explained. Again, the cited references do not mention any asymmetric induction but focus on the effects of stability and veer on the wake morphology.

Reply: We have removed the term "asymmetric induction zone " as the reference stated are primarily discussing the wake shape under wind veer and shear.

Comment 20 — L 453-456: You could cite Fleming et al, 2018 to support the fact that wake rotation and counter-rotating vortices sum up in the positive yaw case and cancel out in the negative one.

Reply: We have added reference to Fleming et al.,2018 and modified the text to the following:

The findings correspond to Fleming et al.,2018, where a stronger wake deflection for positive yaw case is seen due to the aggregated effect of the wake rotation and counter-rotating vortices in comparison to the negative deflection case.

Comment 21 — L 457: Which velocity? The lateral one?

Reply: Here we refer to the longitudinal velocity and have modified the text accordingly.

Comment 22 — Figures 16 and 17: please swap the plots to show first the positive yaw as in Figure 15.

Reply: We have swapped the plots to maintain consistency with Fig. 15.

Comment 23 — L 474-475: It is hard to see the claimed stronger induction for negative y. Maybe provide a quantitative parameter like the velocity ratio between inflow and location closer to rotor plane.

Reply: We estimated the velocity reduction between the most upstream scan location (0.8 D) and very close to the rotor plane ($0D$) by calculating the velocity ratio between the two locations at various spanwise locations given by the following equation:

$$v_{\text{ratio}} = \frac{v_{0.8\text{D}}}{v_{0\text{D}}} \tag{1}$$

For brevity, we show the velocity reduction ratio at spanwise positions $y/D = 0.19$ and $y/D = -0.19$ as the trend remained similar towards the rotor tips. For the positive yaw case, the value of v_{ratio} was 1.2 and 1.14 at $y/D = -0.19$ and $y/D = 0.19$ respectively. Similarly, for the negative yaw case, the value of v_{ratio} was 1.23 and 1.04 at $y/D = -0.19$ and $y/D = 0.19$ respectively. We have added the following text to the revised manuscript:
The induction strength between the left and right sides of the rotor is quantified using the ratio of the longitudinal wind speed far upstream of the scan at 0.8 D and the rotor plane at 0 D as $v_{\text{ratio}} = \frac{v_{0.8\text{D}}}{v_{0\text{D}}}$. For the positive yaw case, the value of v_{ratio} was 1.2 and 1.14 at $y/D = -0.19$ and $y/D = 0.19$ respectively. Similarly for the negative yaw case, the value of v_{ratio} was 1.23 and 1.04 at $y/D = -0.19$ and $y/D = 0.19$ respectively with similar trends observed at other spanwise positions.

Comment 24 — L 477-478: The wake recovery followed by the deceleration is only visible for the positive yaw case.

Reply: We regret that our statement on the paper has been misinterpreted. We have not noted that the wake recovery followed by deceleration was visible in the positive yaw case. We simply wanted to convey that the induction effect is stronger at $y/D < 0$ which was exposed to the wake for the negative yaw case. We have added the following text to the revised manuscript:
For the negative offset case, similar effects of the induction are seen where the wake at $y/D < 0$ decelerated faster compared to the freestream at $y/D > 0$.

Comment 25 — L 496: why is the probe averaging not included as possible source of errors?

Reply: Probe volume averaging is indeed a source of error and we have added this in the revised version.

Comment 26 — L511 - The explanation of the angle of attack as the cause of non-symmetrical induction is not sound (see above). The cited Bastankhah paper shows a symmetrical induction for 0-yaw misalignment (below):

Reply: Bastankah et al [2], in their measurements of a turbine operating with zero yaw noted "a slight lateral asymmetry with respect to the rotor axis" visualised with the iso-velocity contours at far upstream positions ($x/D \approx 1$) with the asymmetry vanishing towards the rotor plane, similar to our measurements.
We have updated the explanation of the non-symmetrical induction to also include the interaction of wind shear with wake rotation and the effect of terrain and the tall tree line.

Comment 27 — L 524-525: the non-symmetrical induction one is hard to see (see above).

Reply: The non-symmetrical induction for the aligned inflow case is visible through the iso-velocity contours at far upstream locations ($x/D \approx 1$) and disappears towards the rotor plane.

Comment 28 — L 550: the explanation of the shear as the cause of non-symmetrical induction is not sound (see above).

Reply: We have updated the explanation of the non-symmetrical induction to also include the interaction of wind shear with wake rotation and the effect of terrain and the tall tree line. We hope that these changes to the manuscript will provide a suitable explanation for the measurements.

References

[1] R. J. Barthelmie. The effects of atmospheric stability on coastal wind climates. *Meteorological Applications*, 6(1):39–47, 3 1999.

[2] M. Bastankhah and F. Porte-Agel. Wind tunnel study of the wind turbine interaction with a boundary-layer flow: Upwind region, turbine performance, and wake region. *Physics of Fluids*, 29(6), 2017.

[3] BKG. Digitales Geländemodell Gitterweite 200 m, 2013.

[4] E. Branlard and A. R. Meyer Forsting. Assessing the blockage effect of wind turbines and wind farms using an analytical vortex model. *Wind Energy*, 23(11):2068–2086, 11 2020.

[5] M. Bromm, A. Rott, H. Beck, L. Vollmer, G. Steinfeld, and M. Kühn. Field investigation on the influence of yaw misalignment on the propagation of wind turbine wakes. *Wind Energy*, 21(11):1011–1028, 11 2018.

[6] J. Counihan, J. C. Hunt, and P. S. Jackson. Wakes behind two-dimensional surface obstacles in turbulent boundary layers. *Journal of Fluid Mechanics*, 64(3):529–564, 1974.

[7] P. Hulsman, C. Sucameli, V. Petrović, A. Rott, A. Gerds, and M. Kühn. Turbine power loss during yaw-misaligned free field tests at different atmospheric conditions. *Journal of Physics: Conference Series*, 2265(3):032074, 5 2022.

[8] H. A. Madsen, V. Riziotis, F. Zahle, M. O. Hansen, H. Snel, F. Grasso, T. J. Larsen, E. Politis, and F. Rasmussen. Blade element momentum modeling of inflow with shear in comparison with advanced model results. In *Wind Energy*, volume 15, pages 63–81. John Wiley and Sons Ltd, 1 2012.

[9] A. R. Meyer Forsting, M. P. Van Der Laan, and N. Troldborg. The induction zone/factor and sheared inflow: A linear connection? In *Journal of Physics: Conference Series*, volume 1037, page 072031. IOP Publishing, 6 2018.

[10] T. Mikkelsen, M. Sjöholm, P. Astrup, A. Peña, G. Larsen, M. F. van Dooren, and A. P. Kidambi Sekar. Lidar Scanning of Induction Zone Wind Fields over Sloping Terrain. *Journal of Physics: Conference Series*, 1452(1):012081, 1 2020.

[11] A. S. Monin and A. M. Obukhov. Basic laws of turbulent mixing in the surface layer of the atmosphere. *Originally published in Tr. Akad. Nauk SSSR Geophiz. Inst*, 24(151):163–187, 1954.

[12] A. Peña and J. Mann. Turbulence Measurements with Dual-Doppler Scanning Lidars. *Remote Sensing*, 11(20):2444, 10 2019.

[13] C. Stawiarski, K. Traumner, C. Knigge, and R. Calhoun. Scopes and challenges of dual-doppler lidar wind measurements-an error analysis. *Journal of Atmospheric and Oceanic Technology*, 30(9):2044–2062, 2013.

[14] N. Tobin, A. M. Hamed, and L. P. Chamorro. Fractional Flow Speed-Up from Porous Windbreaks for Enhanced Wind-Turbine Power. *Boundary-Layer Meteorology*, 163(2):253–271, 5 2017.

[15] M. F. van Dooren, F. Campagnolo, M. Sjöholm, N. Angelou, T. Mikkelsen, and M. Kühn. Demonstration and uncertainty analysis of synchronised scanning lidar measurements of 2-D velocity fields in a boundary-layer wind tunnel. *Wind Energy Science*, 2(1):329–341, 6 2017.

[16] M. F. van Dooren, D. Trabucchi, and M. Kühn. A methodology for the reconstruction of 2D horizontal wind fields of wind turbinewakes based on dual-Doppler lidar measurements. *Remote Sensing*, 8(10):809, 9 2016.